Sonication of proteins causes formation of aggregates that resemble amyloid

PETER B. STATHOPULOS,[1] GUENTER A. SCHOLZ,[2] YOUNG-MI HWANG,[1]
JESSICA A.O. RUMFELDT,[1] JAMES R. LEPOCK,[3] AND ELIZABETH M. MEIERING[1]

[1]Guelph-Waterloo Centre for Graduate Studies in Chemistry and Biochemistry and [2]Department of Physics, University of Waterloo, Waterloo, Ontario N2L 3G1, Canada
[3]Department of Medical Biophysics and Ontario Cancer Institute, University of Toronto, Toronto, Ontario M5G 2M9, Canada

(RECEIVED April 22, 2004; FINAL REVISION July 28, 2004; ACCEPTED August 5, 2004)

Abstract

Despite the widespread use of sonication in medicine, industry, and research, the effects of sonication on proteins remain poorly characterized. We report that sonication of a range of structurally diverse proteins results in the formation of aggregates that have similarities to amyloid aggregates. The formation of amyloid is associated with, and has been implicated in, causing of a wide range of protein conformational disorders including Alzheimer's disease, Huntington's disease, Parkinson's disease, and prion diseases. The aggregates cause large enhancements in fluorescence of the dye thioflavin T, exhibit green-gold birefringence upon binding the dye Congo red, and cause a red-shift in the absorbance spectrum of Congo red. In addition, circular dichroism reveals that sonication-induced aggregates have high β-content, and proteins with significant native α-helical structure show increased β-structure in the aggregates. Ultrastructural analysis by electron microscopy reveals a range of morphologies for the sonication-induced aggregates, including fibrils with diameters of 5–20 nm. The addition of preformed aggregates to unsonicated protein solutions results in accelerated and enhanced formation of additional aggregates upon heating. The dye-binding and structural characteristics, as well as the ability of the sonication-induced aggregates to seed the formation of new aggregates are all similar to the properties of amyloid. These results have important implications for the use of sonication in food, biotechnological and medical applications, and for research on protein aggregation and conformational disorders.

Keywords: sonication; ultrasound radiation; amyloid; fibrils; protein aggregation; β-structure; protein conformational disorder; protein misfolding

Loomis and Wood first reported the damaging effects of ultrasound radiation on biological systems in 1927 (Wood and Loomis 1927). In the intervening years, myriad applications of ultrasound in medicine and industry have been developed; however, the details of ultrasound-induced damage to biomolecules, especially proteins, remain poorly characterized. Such characterization is difficult, owing to the potentially complex mechanisms of sonication-induced damage. These may include the formation of liquid–gas interfaces, local heating effects, mechanical/sheer stresses, and free radical reactions (Hawkins and Davies 2001; Mason and Peters 2002). The functional native structure of proteins is determined by the subtle balance between many noncovalent interactions; this balance can be easily disrupted by the above mechanisms, leading to protein denaturation and aggregation.

Many applications of ultrasound in common use today may alter protein structures (Mason and Peters 2002). For example, sonication is used to prepare proteinaceous micro-

Reprint requests to: Elizabeth M. Meiering, Guelph-Waterloo Centre for Graduate Studies in Chemistry and Biochemistry, University of Waterloo, Waterloo, Ontario N2L 3G1, Canada; e-mail: meiering@uwaterloo.ca; fax: (519) 746-0435.

Abbreviations: ThT, thioflavin T; CR, Congo red; CD, circular dichroism; TEM, transmission electron microscopy; DLS, dynamic light scattering; PMCA, protein misfolding cyclic amplification; SDS-PAGE, sodium dodecyl sulfate polyacrylamide electrophoresis; BSA, bovine serum albumin; SOD, human cytosolic Cu/Zn superoxide dismutase; GSH, reduced glutathione; K_d, apparent dissociation constant.

Article published online ahead of print. Article and publication date are at http://www.proteinscience.org/cgi/doi/10.1110/ps.04831804.

spheres of human serum albumin (Grinstaff and Suslick 1991) (e.g., Albunex and Optison); these are widely used as ultrasound contrast agents, and are being investigated as possible gene transfer vehicles (Li et al. 2003). Sonication is also employed in procedures to encapsulate therapeutic proteins, such as asparaginase, insulin, and erythropoietin, in biodegradable poly(D,L-lactide-co-glycolide) microspheres for controlled release in vivo (Bittner et al. 1998; Jiang et al. 2003; Wolf et al. 2003). These microsphere protein-loading techniques are known to result in some protein inactivity and aggregation (van de Weert et al. 2000). Sonication is also used to sterilize surgical and dental instruments, for dental descaling; in water treatment for inactivation of chemical and biological pollutants; in the food industry for the preparation of emulsions; and in laboratories for cell disruption and, recently, for studies of protein conformational disorders. In these disorders, which include, for example, Alzheimer's disease, Huntington's disease, prion diseases, immunoglobulin light chain disorders and serpinopathies, naturally occurring proteins are altered or mutated, and the variant proteins misfold to form aggregates that may be causative agents in the diseases (Soto 2001; Lomas and Carrell 2002; Stefani and Dobson 2003). Soto and coworkers have reported a new method, termed protein misfolding cyclic amplification (PMCA), for possible diagnosis of prion disorders (Saborio et al. 2001; Soto et al. 2002). In PMCA, tiny quantities of prion aggregates can be detected with high sensitivity by amplifying the aggregates through cycles of sonication (to break existing aggregates into smaller pieces) followed by incubation periods (in which the small aggregates act as seeds for the formation of new aggregate from soluble prion protein). Sonication is also frequently used to break aggregates into smaller pieces for seeding new aggregate growth in laboratory studies of proteins and peptides associated with various conformational disorders, such as Alzheimer's (Jarrett et al. 1993; O'Nuallain et al. 2004), Huntington's (Chen et al. 2001), prion diseases (Saborio et al. 2001; Soto et al. 2002), and serpinopathies (Crowther et al. 2003), as well as non-disease-associated proteins (Jarrett and Lansbury 1992; Ramirez-Alvarado et al. 2000).

Amyloid is a common aggregate structure that has been observed for numerous disease- and nondisease-associated proteins (Stefani and Dobson 2003), and has been proposed to be an alternative structure that may be adopted by all proteins under conditions where the native state is destabilized (Fandrich et al. 2001). We report here that sonication of a range of structurally diverse proteins results in the formation of aggregates that have tinctorial, structural, and seeding properties similar to those of amyloid. These results have important and far-reaching implications for the use of sonication in medicine, biotechnology, and research.

Results

To obtain representative information on the effects of sonication on proteins, a range of unrelated proteins with diverse structures was chosen for study (Table 1). Protein structures included mainly α-helical (bovine serum albumin [BSA], myoglobin), mixed α-helix and β-sheet (lysozyme, Tm0979), and mainly β-sheet (hisactophilin, Cu/Zn superoxide dismutase [SOD]). Cysteine residues are a particularly common site for free radical reactions in proteins

Table 1. *Biochemical data for proteins subjected to sonication*

Protein	Molecular weight[a] (kDa)	Number of disulfides	Number of free thiols	Native secondary structure[b] Alpha (%)	Native secondary structure[b] Beta (%)	Native secondary structure[b] Random (%)	Aggregate secondary structure[b] Alpha (%)	Aggregate secondary structure[b] Beta (%)	Aggregate secondary structure[b] Random (%)	ThT increase[c] (fold)	CR shift[d] (nm)
BSA	66.4	17	1	74	11	14	38	35	26	12	528
Myoglobin	17.0	0	0	66	17	16	48	28	23	2.2	543
Lysozyme	14.6	4	0	29	42	28	16	54	31	5.4	543
Tm0979	24.0	0	0	10	57	32	10	59	31	38	526
SOD	31.8	2	0	8	59	32	9	60	31	5.3	522
Hisactophilin	13.7	0	1	6	61	32	7	61	32	29	543

[a] MW for native proteins, which are all monomers except for SOD and Tm0979, which are dimers. The pdb codes for the proteins are 1AO6 for human serum albumin (structure for BSA has not been reported), 1WLA for myoglobin, 1E8L for lysozyme, 1X9A for Tm0979, 1HCE for hisactophilin, and 1SOS for SOD.

[b] Percent secondary structure was estimated on DICHROWEB using the CDSSTR method (Sreerama and Woody 2000; Lobley et al. 2002); beta = (β-strands + β-turns). Changes in β-structure for BSA, myoglobin, and lysozyme are predominantly due to augmented β-strand levels (>54, 73, and 92%, respectively).

[c] ThT increase was determined by dividing the fluorescence intensity at the maximum wavelength for the sonicated protein spectra by the fluorescence intensity of the native protein spectra at the same wavelength.

[d] CR shift was determined by subtracting the native protein spectra from the sonicated protein spectra and determining the points of maximal spectral difference.

(Hawkins and Davies 2001), and play a central role in the sonication-induced formation of human serum albumin proteinaceous microspheres (Grinstaff and Suslick 1991). Thus, proteins were chosen to have different cysteine contents (Table 1): no cysteine (myoglobin, Tm0979), 1 free thiol and 0 or 17 disulfides (hisactophilin and BSA), and no free thiols and 2 or 4 disulfides (SOD and lysozyme). The effects of sonication were characterized by light scattering, binding of the dyes thioflavin T (ThT) and Congo red (CR), measurements of protein secondary structure using circular dichroism (CD) spectropolarimetry, determination of ultrastructure using transmission electron microscopy (TEM), assessing aggregate stability by denaturing gel electrophoresis (SDS-PAGE), and examining the seeding ability of sonicated protein solutions.

Cycle-dependence of aggregation

The conditions used herein for sonication were similar to those used in the PMCA methodology (Saborio et al. 2001; Soto et al. 2002); proteins were typically subjected to 40 cycles of sonication (5 pulses of 1 sec) followed by incubation periods (1 min). After 40 rounds of sonication, small amounts of visible precipitate were observed in all the protein solutions. Using this protocol >90% of the protein remained in solution after sonication, based on measurements of supernatant protein concentration after centrifugation of sonicated solutions. The relationship between the extent of sonication and amount of protein aggregation was investigated by measuring 90° light-scattering intensity and ThT binding as a function of number of sonication cycles (Fig. 1). The formation of protein aggregates that are large relative to the wavelength of incident light results in scattering of light; aggregate formation can also be monitored by enhanced fluorescence upon binding of ThT (see following section). A linear dependence was observed between light-scattering intensity and the number of sonication cycles or ThT fluorescence (Fig. 1A,B), suggesting that the amount of sonication-induced aggregation is proportional to the extent of the sonication treatment. To investigate the contribution of aggregate size to the total light scattering intensity as a function of sonication cycle number, additional dynamic light scattering (DLS) and TEM experiments were performed. The distribution of particle sizes measured by DLS (Fig. 1C) and the particle sizes and morphologies observed by TEM (data not shown) do not change significantly above 5 sonication cycles, consistent with amount of aggregate formation being proportional to the number of sonication cycles.

Thioflavin T and Congo red binding to aggregates

ThT (LeVine 1999) and CR (Klunk et al. 1999) are standard dyes used to monitor the formation of amyloid structure.

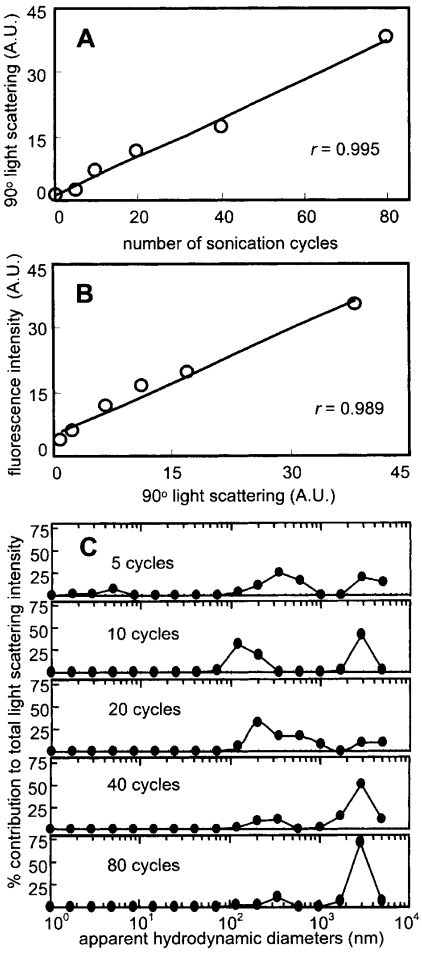

Figure 1. (*A*) Cycle number-dependence of sonication-induced protein aggregation of BSA. Light scattering increased in a linear fashion with increasing number of sonication cycles from 0 to 80 cycles ($r = 0.995$). (*B*) Correlation between ThT fluorescence and light scattering for BSA. ThT fluorescence increased in a strong linear fashion with amount of protein aggregate as determined by light scattering ($r = 0.989$). (*C*) Distribution of apparent hydrodynamic diameters of BSA as a function of sonication cycle number as determined by DLS. The unsonicated protein solution had a relatively low polydispersity with an effective diameter of ~3 nm, as expected for monomeric BSA. At 5 cycles, correlation function deconvolution shows the persistence of a distribution corresponding to monomeric BSA along with a larger aggregate distribution (>100 nm). The range of sizes is relatively unchanged between 10 and 80 cycles.

Amyloid binding to ThT causes a marked enhancement of ThT fluorescence, while binding to CR causes a red shift in the absorbance spectrum of the dye and green-gold birefringence of aggregates under polarized light. ThT fluorescence of amyloid is typically measured using an excitation wavelength of 440 nm, giving an emission maximum at ~482 nm. The proteins studied here do not absorb significantly in this wavelength range, except for myoglobin, in which the heme cofactor has significant absorbance (maximum at 407–410 nm). As a consequence, ThT fluorescence enhancement for myoglobin may be underestimated; consistent with this, the

fluorescence values for both unsonicated and sonicated myoglobin are relatively low (Fig. 2; Table 1). Sonication caused significant enhancement of ThT fluorescence for all the proteins studied, ranging from 2.2-fold enhancement for myoglobin to 38-fold for Tm0979 (Fig. 2; Table 1). These enhancements are comparable to the 2–60-fold enhancements reported for amyloid and other amyloid-like fibrils (Ismail et al. 1992; LeVine 1993; Schmittschmitt and Scholtz 2003).

To investigate whether the different levels of ThT enhancement are related to a different mode of ThT binding by different aggregates, a ThT titration was conducted on aggregates of an all-α protein (BSA) and an all-β protein (SOD) (Fig. 3). The titration data transformed as Scatchard plots are linear for aggregates of both proteins, consistent with a single type of binding site in both cases. The apparent dissociation constants (K_d) and magnitudes of the fluorescence enhancements for both proteins agree within an order of magnitude, suggestive of roughly similar binding modes. Interestingly, however, ThT appears to bind more tightly upon binding to aggregates of the all-β protein.

Bright-field microscopy of aggregates treated with CR showed that aggregates of all the proteins bind the dye (Fig. 4, left panels) and exhibit birefringence under cross-polarized light (Fig. 4, right panels). The birefringence varies somewhat in color, but is often green-gold, as is characteristic for CR binding to amyloid (Westermark et al. 1999). Upon incubation of protein solutions for longer periods of time after sonication, further aggregate assembly was observed, as evidenced by increased formation of large tangles

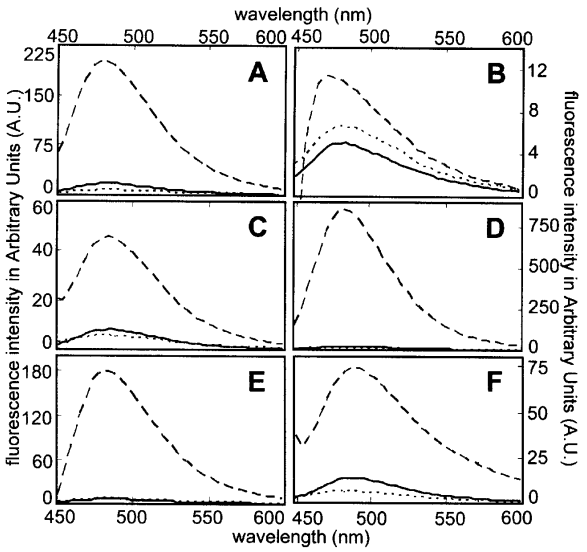

Figure 2. ThT fluorescence enhancement properties of sonicated proteins. ThT fluorescence emission spectra are shown for solutions with no added protein (···), native protein at 1 mg/mL (———), or sonicated protein at 1 mg/mL (– – –). (*A*) BSA. (*B*) Myoglobin. (*C*) Lysozyme. (*D*) Tm0979. (*E*) Hisactophilin. (*F*) SOD.

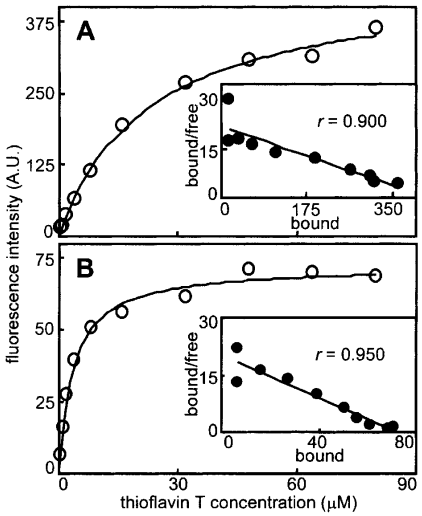

Figure 3. ThT binding properties of sonicated proteins. ThT titration curves are shown for sonicated protein solutions at 0.1 mg/mL (open circles). The solid lines represent the hyperbolic fits to the data. *Insets* are Scatchard-like transformations of the data (filled circles). Scatchard data were fit well by linear regression (solid lines) for both (*A*) BSA ($r = 0.900$) and (*B*) SOD ($r = 0.950$). Apparent K_d values determined by both analyses indicate a greater affinity of ThT for SOD (an all-β native protein) than for BSA (an all-α native protein) (K_d of 3.5 μM vs. 22 μM, respectively).

of fibrillar aggregates with strong birefringence (Fig. 4G–I), with a concomitant decrease in sample turbidity. The more pronounced birefringence in these samples is likely due to the changes in sample thickness, which is a critical determinant of CR birefringence (Wolman and Bubis 1965). Spectral shifts for CR upon aggregate binding were found to be maximal at 526–543 nm (Fig. 5; Table 1). These shifts are similar to the characteristic maximum difference at ~541 nm observed for amyloid (Klunk et al. 1999), and the differential absorbance values are comparable to levels observed for other amyloid and amyloid-like fibrils (Gross et al. 1999; Chiti et al. 2001; Sirangelo et al. 2002; Koscielska-Kasprzak and Otlewski 2003).

Secondary structure of aggregates

Amyloid has a characteristic "cross-β" structure, in which a fibrillar structure is formed by β-strands that run perpendicular to the axis of the fibril (Sunde and Blake 1997). A change in CD spectrum characteristic of increased β-structure has been observed when various native proteins, including myoglobin (Fandrich et al. 2001) and lysozyme (Goda et al. 2000), convert to an amyloid structure. Secondary structure analysis of CD spectra of the native proteins studied here and of the aggregates formed after sonication is given in Table 1. For the proteins that contain substantial helical structure in the native state (myoglobin,

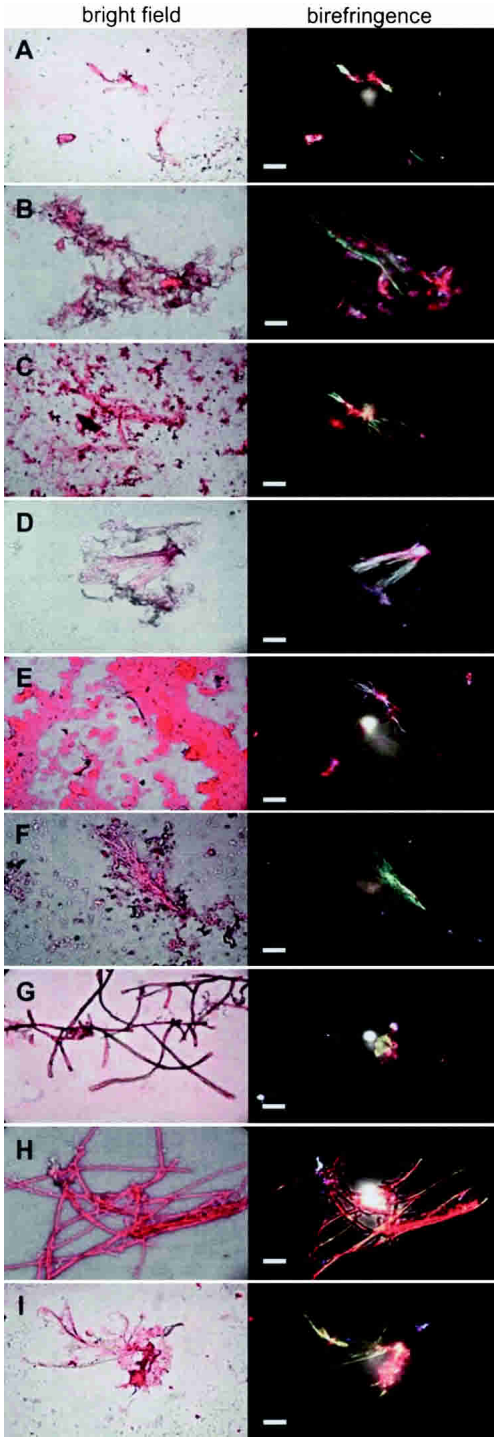

Figure 4. CR birefringence of sonicated proteins. Bars are 100 μm. *A–F* are CR samples prepared on the same day that proteins were sonicated; *G–I* were prepared after incubating sonicated proteins at ambient temperature for 14, 5, and 30 d, respectively. (*A*) BSA. (*B*) Myoglobin. (*C*) Lysozyme. (*D*) Tm0979. (*E*) Hisactophilin. (*F*) SOD. (*G*) BSA. (*H*) Tm0979. (*I*) Hisactophilin. Continued assembly was apparent for all the sonication-induced aggregates; however, the BSA, Tm0979, and hisactophilin (*G–I*) samples were the most marked by Congo red polarizing light microscopy.

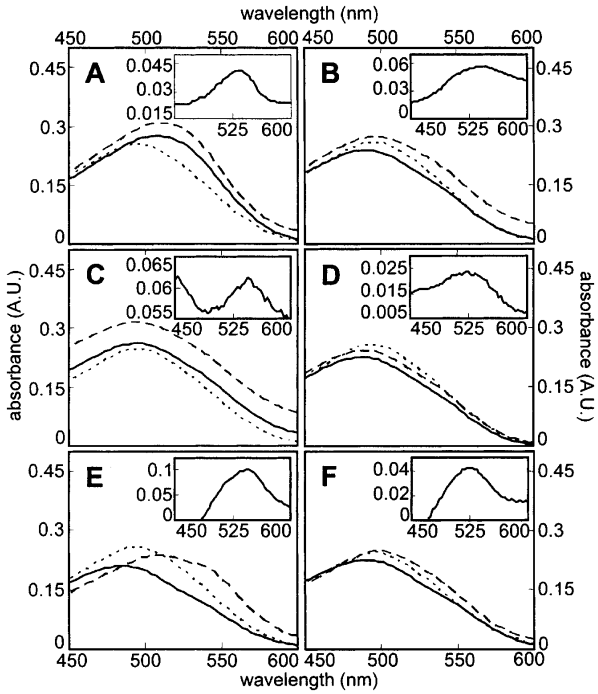

Figure 5. Spectral shifts induced in CR by sonicated proteins. CR absorbance spectra acquired with a 0.3-cm path length cuvette are shown for solutions with no added protein (···) and solutions containing native (———) or sonicated (– – –) protein at 1 mg/mL. *Insets* show difference spectra obtained by subtracting the spectra of native protein solutions from those of sonicated protein solutions. (*A*) BSA. (*B*) Myoglobin. (*C*) Lysozyme. (*D*) Tm0979. (*E*) Hisactophilin. (*F*) SOD.

BSA, and lysozyme), sonication causes an increase in β-structure with a concomitant decrease in α-helical structure. For the proteins with predominantly β-features in native CD spectra (SOD, hisactophilin, Tm0979), spectral changes upon sonication are less pronounced, and there is little apparent change in secondary structure.

Ultrastructure of aggregates

The ultrastructure of the sonication-induced aggregates was investigated by TEM; typical structures are shown in Figure 6. For all the proteins studied, the aggregates exhibit a range of morphologies, including apparently amorphous structures (Fig. 6, left panels) and fibrillar species (Fig. 6, right panels). The structures of these aggregates have a strong resemblance to structures reported for other unsonicated and sonicated amyloid aggregates (O'Nuallain et al. 2004). Fibril diameters are typically between ~5 and 20 nm (Fig. 6, right panels), and fibrils are often observed in bundles (Fig. 6D–F). Within the 20 nm fibrils, coiling together of thinner fibrils is often apparent. These structures and diameters are similar to those reported for amyloid fibrils (Sunde and Blake 1997).

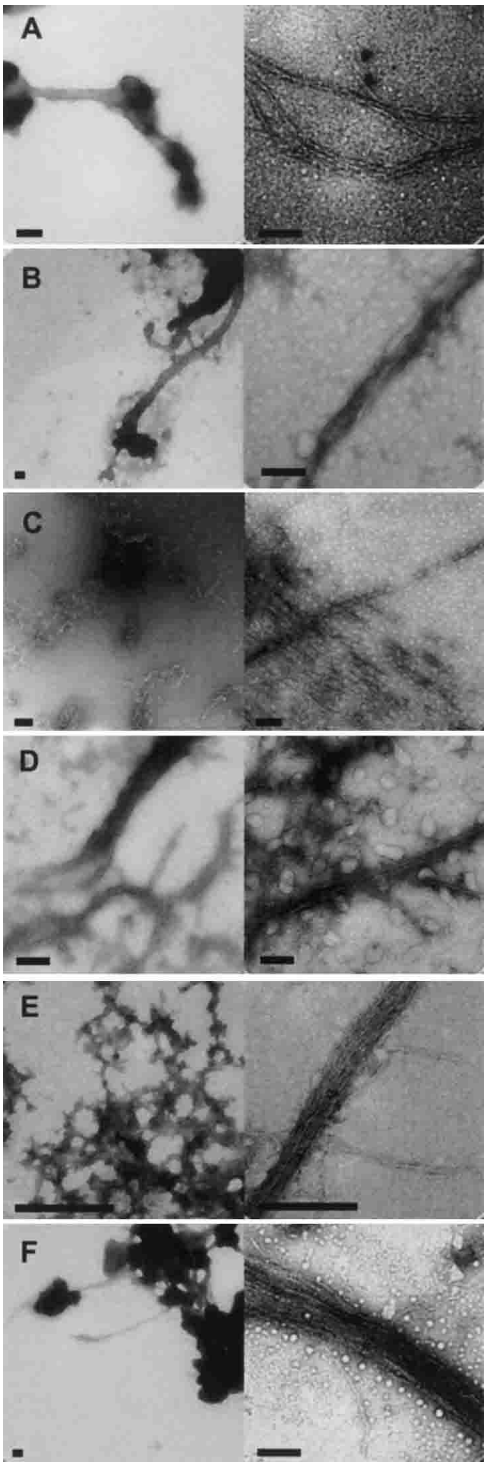

Figure 6. TEM of representative sonication-induced amorphous (*left*) and fibrillar (*right*) aggregates. Bars are 200 nm. (*A*) BSA. (*B*) Myoglobin. (*C*) Lysozyme. (*D*) Tm0979. (*E*) Hisactophilin. (*F*) SOD.

Aggregate stability

Amyloid fibrils and associated structures are generally very stable and resistant to resolubilization through various physical and chemical treatments, such as heat, reducing agents, and detergents (Glover et al. 1997; Scherzinger et al. 1997; Tanaka et al. 2002; Stefani and Dobson 2003). The aggregates formed here by sonication also appear to be very stable. Aggregates pelleted by centrifugation and resuspended in buffer did not redissolve over a timescale of weeks. The stability of pelleted aggregates was also tested by SDS-PAGE of samples boiled in buffer containing 7 M urea, 2% (w/v) of the detergent SDS, and in the presence and absence of the reducing agent, 5% (v/v) β-mercaptoethanol. Substantial quantities of aggregate did not redissolve, and could be observed visually in the boiled samples. There appeared to be some limited resolubilization of the aggregates, because weak bands were observed at molecular weights corresponding to the monomer, after silver staining (data not shown). However, the observed monomeric bands may have been the result of protein adhering to or trapped within pellets, despite extensive washing prior to experiments.

Seeding with sonicated protein

Amyloid aggregates have been shown to act as seeds for the formation of new aggregate from soluble protein (Rochet and Lansbury 2000). In general, seeding effects tend to increase with increasing temperature, although they have been reported to decrease again at temperatures well above the thermal melting points of proteins (Ramirez-Alvarado et al. 2000; Fandrich et al. 2003). Seeding of further aggregate formation by sonication-induced aggregates was investigated by incubating native proteins at various temperatures in the presence and absence of aggregates and monitoring aggregate formation by ThT fluorescence (Fig. 7). Small increases in ThT fluorescence were observed for proteins incubated in the absence of aggregates; this is consistent with previous studies showing formation of amyloid at elevated temperatures by various proteins including myoglobin (Fandrich et al. 2003) and lysozyme (Morozova-Roche et al. 2000). When proteins were incubated in the presence of aggregates, the increases in ThT fluorescence were larger in magnitude and occurred more rapidly than in the absence of aggregates (Fig. 7). The enhancement and acceleration of aggregation generally increased with increasing temperature at temperatures below the thermal melting point of the proteins, and then decreased as temperature was increased further. Thus, sonication-induced aggregates appear to seed the formation of further amyloid-like aggregates from soluble protein in a similar way to that observed for amyloid aggregates.

Discussion

Does sonication induce formation of amyloid?

Based on various probes of structure (binding of ThT and CR, CD, and TEM) the sonication of many different pro-

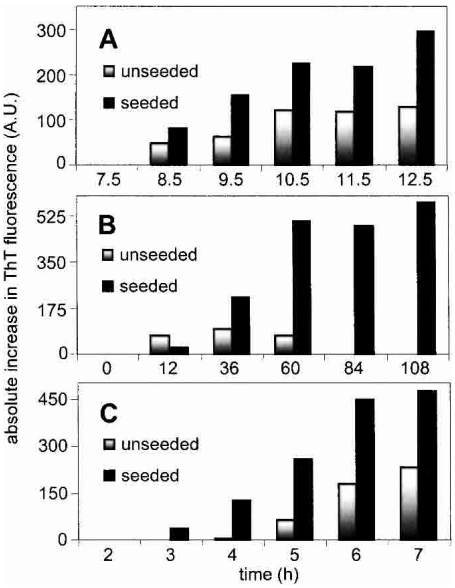

Figure 7. Seeding characteristics of sonication-induced aggregates. (*A*) BSA, (*B*) myoglobin, and (*C*) lysozyme, incubated at 50°C, 45°C, and 65°C, respectively, with corresponding apparent maxima for differential scanning calorimetry thermal unfolding transitions of unsonicated native protein being 64°C, 80°C, and 73°C. Seeded samples (black bars) exhibited a greater absolute increase in ThT binding and fluorescence as well as more rapid increase in ThT fluorescence compared to the unseeded samples (gray bars).

teins results in the formation of aggregates with properties similar to those of amyloid. Furthermore, the sonication-induced aggregates resemble amyloid with respect to their high stability against resolubilization upon treatment with heat, detergent, and reducing agent (Glover et al. 1997; Scherzinger et al. 1997; Tanaka et al. 2002; Stefani and Dobson 2003), and their ability to enhance and accelerate further aggregation (Harper and Lansbury 1997). These are striking results, particularly considering that the proteins studied have unrelated and diverse sequences and structures. It should be noted that, given the low resolution of the structural probes and the range of aggregate morphologies observed by TEM, there may be considerable variability in the structural details of the aggregates formed by the different proteins, and not all of the aggregates formed within each sample are necessarily amyloid-like. Also, it has been shown that various types of aggregates have high β-sheet content, which may or may not be related to the β-structure found in amyloid (Fink 1998; Dong et al. 2000). The characterization of amyloid and other aggregate structures is difficult because these species are not readily amenable to high resolution structural analysis and are often heterogeneous; however, the data obtained here using various standard measures of amyloid formation are consistent with sonication causing significant formation of amyloid aggregate. Furthermore, the formation of amyloid by many different proteins upon sonication is consistent with the fact that a large number of proteins with diverse structures, including both disease and nondisease associated proteins, are able to form amyloid (Stefani and Dobson 2003).

Mechanisms of sonication-induced protein aggregation

Amyloid has been proposed to be a generic structure that can be adopted by all proteins under conditions where the native state is destabilized (Fandrich et al. 2001). Partial or complete unfolding of the native state is generally believed to be required for amyloid formation (Fink 1998; Kelly 1998; Rochet and Lansbury 2000; Fandrich et al. 2003). Amyloid formation in vitro can be enhanced by decreasing protein stability through changes in protein covalent structure, increased temperature, extreme pH, and addition of alcohols. Similarly, sonication may also enhance unfolding and amyloid formation by destabilizing proteins through various chemical and physical processes.

Sonication produces gas bubbles which collapse, in a process known as cavitation, creating extremely high local temperatures, high sheer forces, and the free radicals H· and OH· from sonolysis of water. Proteins may be destabilized at the air–liquid interface of sonication-induced bubbles (Satheeshkumar and Jayakumar 2002). The extremely reactive OH· radical undergoes various reactions resulting in formation of other reactive oxygen species, such as H_2O_2 and O_2^-. Reactive oxygen species react with many different chemical moieties on proteins, producing protein radicals, which then undergo further reactions such as oxidation, chain reactions, crosslinking, and cleavage reactions (Hawkins and Davies 2001), which are likely to decrease protein stability. Formation of nonnative disulfide bonds is one example of a destabilizing chemical modification (Senisterra et al. 1997) that may be particularly relevant for amyloid formation (Lee and Eisenberg 2003). In preliminary experiments, the effects of free radical reactions were investigated by sonicating hisactophilin and BSA, which both contain a single free thiol and either zero or 17 disulfide linkages, respectively (Table 1), in the presence of the cellular free radical scavenger, reduced glutathione (GSH). With GSH present, aggregation was significantly decreased for hisactophilin, but not for BSA (data not shown). This suggests some involvement of free radical reactions in aggregate formation for at least some proteins.

Additional consequences of sonication that may cause protein unfolding and enhance aggregation are high temperature and mechanical forces (Mason and Peters 2002). Physical shearing may disrupt the native fold but leave secondary structural elements intact (Carrion-Vazquez et al. 2000) and thereby enhance intermolecular interactions and aggregation. Significant secondary structural change upon sonication-induced aggregation is not observed by CD for proteins with high levels of β-structure, while native α-helical proteins undergo a conversion to increased β-structure

upon aggregation. Sonication-induced aggregation of the all-β proteins examined may involve the unfolding of protective features, uncovering of β-strands, and association of these exposed strands into aggregates, while α-helical proteins may undergo a more significant rearrangement in secondary structure upon aggregation. The requirement of α-helical proteins to undergo major structural changes upon amyloid-like aggregation may contribute to the apparent differences in ThT affinity and fluorescence enhancement between aggregates from α-helical and β-sheet proteins. Studies are in progress to investigate this phenomenon further.

Some of the proteins studied here have been found previously to form aggregates that may resemble amyloid. Heating causes increased β-structure formation and gelation for BSA (Clark et al. 1981b), lysozyme (Clark et al. 1981b), and myoglobin (Dong et al. 2000; Meersman et al. 2002). TEM characterization of protein gels has revealed a range of structures, including networks of fibrils (Clark et al. 1981a; Kavanagh et al. 2000). Cysteine-mediated free radical reactions induced by ultraviolet light also result in gelation and increased β-sheet formation for BSA (Wei et al. 2003). Lysozyme has been shown to form amyloid fibrils upon heating at low pH (Krebs et al. 2000) and addition of ethanol (Goda et al. 2000), and myoglobin also forms amyloid fibrils upon heating at high pH (Fandrich et al. 2001). The common aspect in all of these studies is that aggregation, gelation, and/or fibril formation occur under conditions where the native state is destabilized. This suggests that sonication may also cause formation of amyloid-like aggregates due to protein destabilization through the various physical and chemical mechanisms discussed above. Studies are needed to elucidate further details of the mechanisms involved in sonication-induced aggregation.

Implications of sonication-induced protein aggregation

This study has important and far-reaching implications for the use of ultrasound in research and in medical and biotechnological applications. Different types of amyloid structures, for example in prion strains (Prusiner 1998; Uptain and Lindquist 2002), as well as aggregates distinct from amyloid, for example in serpinopathies (Lomas and Carrell 2002), are biologically relevant. When employing sonication to study protein misfolding, care must be taken to avoid generating potentially irrelevant amyloid-like structures. Once generated, such aggregates may induce the formation of further aggregates with the same structural characteristics, as has been proposed to occur in different mammalian and yeast prion strains (Prusiner 1998; Uptain and Lindquist 2002). For the proteins studied here, there is evidence for further assembly of sonication-induced aggregates with time and for acceleration of aggregation of native protein by sonication-induced aggregates. If further assembly of sonication-induced aggregates or seeding of further aggregation by sonication-induced aggregates can also occur in vivo, this may give rise to immunogenicity, toxicity, or even disease. For proteinaceous and protein-loaded microspheres, purification procedures relying on centrifugation, dialysis, or filtration (Wong and Suslick 1995; Zambaux et al. 1999; Avivi et al. 2001; Kang and Singh 2003) may be ineffective at removing aggregates similar in size to microspheres, covalently linked to microspheres or trapped within microspheres. Therefore, care should be taken to monitor and control the formation of aggregates when employing sonication for basic research, food, biotechnology, and medical applications.

Materials and methods

Reagents

CR, ThT, horse heart myoglobin and hen egg white lysozyme were purchased from Sigma. HEPES and BSA were from BioShop. Recombinant hisactophilin and human cytosolic SOD were prepared as described previously (Liu et al. 2001; Stathopulos et al. 2003). Tm0979 is a predicted protein from *Thermotoga maritima* (Nelson et al. 1999). It was expressed with a 20 amino acid affinity-tag in BL21-(Gold λDE3) *Escherichia coli* cells, and purified by cell lysis through a french press, followed by nickel column affinity chromatography at pH 8.5 (Yee et al. 2002). The purified Tm0979 was then concentrated and exchanged into water by ultrafiltration, flash frozen, and stored at −80°C.

Sonication

Filtered (20 nm filter, Anatop 10, Whatman Ltd.) protein solutions were prepared at 3 mg/mL in 20 mM HEPES (pH 7.8), then sonicated using a W 225R probe sonicator with a standard tapered microtip attached to a 1/2″ disruptor horn (Heat Systems, Ultrasonics, Inc.). The instrument frequency was 20 kHz, and the power output was set to deliver a maximum of 30 watts. Solutions were sonicated at ambient temperature for 5 to 80 cycles, where each cycle consisted of 5 pulses of 1 sec followed by 1-min incubation time at ambient temperature. All experiments were performed within 20 min following the sonication procedure, unless otherwise stated.

Static and dynamic light scattering

Ninety degree light-scattering measurements on samples diluted to 1 mg/mL in 20 mM HEPES (pH 7.8) were performed at 445 nm using excitation and emission slit widths of 1 and 5 nm, respectively, on a Fluorolog3-22 spectofluorometer (Jobin Yvon-Spex, Instruments S.A., Inc.). DLS measurements were made on a Brookhaven 90 Plus particle sizer (Brookhaven Instruments, Inc.). The wavelength of incident light was 678 nm, with a nominal power of 20 mW, and a scattering angle of 90°. Samples were analyzed at 1 mg/mL, 20 mM HEPES (pH 7.8), 25°C. Three correlation functions, each being the average of 10 consecutive measurements, were deconvoluted using the cumulants (quadratic) method (Koppel 1972) for apparently monodisperse solutions (0 sonication cycles) or using the CONTIN method (Provencher

1982) for polydisperse solutions (5 to 80 sonication cycles). Correlation functions were fit using a measured baseline and a distribution of hydrodynamic diameters between 0.5 to 5000 nm.

Thioflavin T enhancement

Samples were diluted to 1 mg/mL protein in 75 μM ThT, 20 mM HEPES (pH 7.8), and fluorescence emission spectra were acquired immediately using an excitation wavelength of 440 nm and excitation and emission slit widths of 1 and 5 nm, respectively. Spectra of samples with no ThT were subtracted from the spectra for corresponding samples containing ThT. Sonicated protein at 0.1 mg/mL was titrated with ThT, and the data were fit to a hyperbolic function using Microcal Origin 5.0 (Microcal Software, Inc.), where the measured fluorescence intensity = ([ThT] × fluorescence maximum)/([ThT] + K_d). Scatchard-like plots were prepared by assuming that nearly all of the ThT was in an unbound form and that all bound ThT molecules had the same fluorescence, as previously described (Naiki et al. 1989). Hence, bound/free was represented as fluorescence intensity divided by total ThT concentration. Apparent K_d values obtained from the hyperbolic data fits were confirmed by linear regression of the transformed data, where $K_d = -1$/slope. Data were acquired using a Fluorolog3-22 spectofluorometer (Jobin Yvon-Spex, Instruments S.A., Inc.) at 25°C.

Congo red birefringence

Protein solutions diluted to 1 mg/mL were incubated in 50 μM CR (Chiti et al. 2001; Srisailam et al. 2002; Bouma et al. 2003), 20 mM HEPES (pH 7.8) for 2 h, then centrifuged for 10 min at 16,000*g*. Pellets were resuspended in water and 10 μL of the suspension were air dried on a glass microscope slide. Specimens were viewed at 400× magnification with a Nikon E400 polarizing microscope. Digitized images were obtained using a Nikon COOLPIX 995 digital camera.

Congo red spectral shift

Protein solutions diluted to 1 mg/mL were incubated in 50 μM CR (Chiti et al. 2001; Sirangelo et al. 2002; Srisailam et al. 2002), 20 mM HEPES (pH 7.8) for 20 min. Absorption spectra were acquired using a Cary 1Bio UV/visible spectrophotometer (Varian) at 25°C and a scan rate of 300 nm/min with a 0.3-cm path length cuvette. For all samples, spectra of corresponding solutions without CR were used as blanks.

Circular dichroism

Protein solutions were prepared at final concentrations of 1 or 2 mg/mL in 5 mM HEPES (pH 7.8). Aggregate solutions were prepared by centrifuging sonicated protein solutions at 16,000*g* for 10 min and resuspending the resulting pellets in water. Data were obtained using a J715 CD spectropolarimeter (Jasco), at 25°C, with a 0.01-cm path length cell, a 50-nm/min scan rate and a 2-nm bandwidth. Spectra were an average of 25 scans from 178 to 260 nm. Secondary structure was estimated on the DICHROWEB Web site using the CDSSTR method (Sreerama and Woody 2000; Lobley et al. 2002).

Transmission electron microscopy

Sonicated protein solutions at 0.1 mg/mL were incubated on 400-mesh carbon-coated formvar copper grids (Marivac, St. Laurent, Quebec) for 6 min. Excess solution was drawn off using filter paper, grids were air dried, then stained for 5 sec with 2% (w/v) uranyl acetate. Specimens were viewed with a Philips CM20 electron microscope at an accelerating voltage of 200 kV. Images were digitized using a Gatan 679 slow-scan CCD camera and analyzed using DIGITALMICROGRAPH (version 2.1, Gatan).

Seeding experiments

Filtered control solutions contained 3 mg/mL protein in 20 mM HEPES (pH 7.8). These solutions were seeded with 20% (v/v) sonicated protein solution. Samples were agitated continuously using a magnetic stir bar during incubation at various temperatures. Aggregation was monitored by removing aliquots, adding ThT to a final concentration of 75 μM, and measuring fluorescence immediately, as described above. The apparent melting point for thermal unfolding transitions was determined by differential scanning calorimetry of the control protein solutions.

Acknowledgments

This research was funded by NSERC Canada, and the Neuromuscular Research Partnership, an initiative of the ALS Society of Canada, MDC and CIHR.

References

Avivi, S., Felner, I., Novik, I., and Gedanken, A. 2001. The preparation of magnetic proteinaceous microspheres using the sonochemical method. *Biochim. Biophys. Acta* **1527:** 123–129.

Bittner, B., Morlock, M., Koll, H., Winter, G., and Kissel, T. 1998. Recombinant human erythropoietin (rhEPO) loaded poly(lactide-co-glycolide) microspheres: Influence of the encapsulation technique and polymer purity on microsphere characteristics. *Eur. J. Pharm. Biopharm.* **45:** 295–305.

Bouma, B., Kroon-Batenburg, L.M., Wu, Y.P., Brunjes, B., Posthuma, G., Kranenburg, O., de Groot, P.G., Voest, E.E., and Gebbink, M.F. 2003. Glycation induces formation of amyloid cross-β structure in albumin. *J. Biol. Chem.* **278:** 41810–41819 [Epub 42003 Aug 41818].

Carrion-Vazquez, M., Oberhauser, A.F., Fisher, T.E., Marszalek, P.E., Li, H., and Fernandez, J.M. 2000. Mechanical design of proteins studied by single-molecule force spectroscopy and protein engineering. *Prog. Biophys. Mol. Biol.* **74:** 63–91.

Chen, S., Berthelier, V., Yang, W., and Wetzel, R. 2001. Polyglutamine aggregation behavior in vitro supports a recruitment mechanism of cytotoxicity. *J. Mol. Biol.* **311:** 173–182.

Chiti, F., Bucciantini, M., Capanni, C., Taddei, N., Dobson, C.M., and Stefani, M. 2001. Solution conditions can promote formation of either amyloid protofilaments or mature fibrils from the HypF N-terminal domain. *Protein Sci.* **10:** 2541–2547.

Clark, A.H., Judge, F.J., Richards, J.B., Stubbs, J.M., and Suggett, A. 1981a. Electron microscopy of network structures in thermally-induced globular protein gels. *Int. J. Pept. Protein Res.* **17:** 380–392.

Clark, A.H., Saunderson, D.H., and Suggett, A. 1981b. Infrared and laser-Raman spectroscopic studies of thermally-induced globular protein gels. *Int. J. Pept. Protein Res.* **17:** 353–364.

Crowther, D.C., Serpell, L.C., Dafforn, T.R., Gooptu, B., and Lomas, D.A. 2003. Nucleation of α 1-antichymotrypsin polymerization. *Biochemistry* **42:** 2355–2363.

Dong, A., Randolph, T.W., and Carpenter, J.F. 2000. Entrapping intermediates of thermal aggregation in α-helical proteins with low concentration of guanidine hydrochloride. *J. Biol. Chem.* **275:** 27689–27693.

Fandrich, M., Fletcher, M.A., and Dobson, C.M. 2001. Amyloid fibrils from muscle myoglobin. *Nature* **410:** 165–166.

Fandrich, M., Forge, V., Buder, K., Kittler, M., Dobson, C.M., and Diekmann, S. 2003. Myoglobin forms amyloid fibrils by association of unfolded polypeptide segments. *Proc. Natl. Acad. Sci.* **100:** 15463–15468.

Fink, A.L. 1998. Protein aggregation: Folding aggregates, inclusion bodies and amyloid. *Fold. Des.* **3:** R9–R23.

Glover, J.R., Kowal, A.S., Schirmer, E.C., Patino, M.M., Liu, J.J., and Lindquist, S. 1997. Self-seeded fibers formed by Sup35, the protein determinant of [PSI+], a heritable prion-like factor of *S. cerevisiae*. *Cell* **89:** 811–819.

Goda, S., Takano, K., Yamagata, Y., Nagata, R., Akutsu, H., Maki, S., Namba, K., and Yutani, K. 2000. Amyloid protofilament formation of hen egg lysozyme in highly concentrated ethanol solution. *Protein Sci.* **9:** 369–375.

Grinstaff, M.W. and Suslick, K.S. 1991. Air-filled proteinaceous microbubbles: Synthesis of an echo-contrast agent. *Proc. Natl. Acad. Sci.* **88:** 7708–7710.

Gross, M., Wilkins, D.K., Pitkeathly, M.C., Chung, E.W., Higham, C., Clark, A., and Dobson, C.M. 1999. Formation of amyloid fibrils by peptides derived from the bacterial cold shock protein CspB. *Protein Sci.* **8:** 1350–1357.

Harper, J.D. and Lansbury Jr., P.T. 1997. Models of amyloid seeding in Alzheimer's disease and scrapie: Mechanistic truths and physiological consequences of the time-dependent solubility of amyloid proteins. *Annu. Rev. Biochem.* **66:** 385–407.

Hawkins, C.L. and Davies, M.J. 2001. Generation and propagation of radical reactions on proteins. *Biochim. Biophys. Acta* **1504:** 196–219.

Ismail, A.A., Mantsch, H.H., and Wong, P.T. 1992. Aggregation of chymotrypsinogen: Portrait by infrared spectroscopy. *Biochim. Biophys. Acta* **1121:** 183–188.

Jarrett, J.T. and Lansbury Jr., P.T. 1992. Amyloid fibril formation requires a chemically discriminating nucleation event: Studies of an amyloidogenic sequence from the bacterial protein OsmB. *Biochemistry* **31:** 12345–12352.

Jarrett, J.T., Berger, E.P., and Lansbury Jr., P.T. 1993. The carboxy terminus of the β amyloid protein is critical for the seeding of amyloid formation: Implications for the pathogenesis of Alzheimer's disease. *Biochemistry* **32:** 4693–4697.

Jiang, G., Qiu, W., and DeLuca, P.P. 2003. Preparation and in vitro/in vivo evaluation of insulin-loaded poly(acryloyl-hydroxyethyl starch)-PLGA composite microspheres. *Pharm. Res.* **20:** 452–459.

Kang, F. and Singh, J. 2003. Conformational stability of a model protein (bovine serum albumin) during primary emulsification process of PLGA microspheres synthesis. *Int. J. Pharm.* **260:** 149–156.

Kavanagh, G.M., Clark, A.H., and Ross-Murphy, S.B. 2000. Heat-induced gelation of globular proteins: Part 3. Molecular studies on low pH β-lactoglobulin gels. *Int. J. Biol. Macromol.* **28:** 41–50.

Kelly, J.W. 1998. The alternative conformations of amyloidogenic proteins and their multi-step assembly pathways. *Curr. Opin. Struct. Biol.* **8:** 101–106.

Klunk, W.E., Jacob, R.F., and Mason, R.P. 1999. Quantifying amyloid by congo red spectral shift assay. *Methods Enzymol.* **309:** 285–305.

Koppel, D.E. 1972. Analysis of macromolecular polydispersity in intensity correlation spectroscopy: The method of cumulants. *J. Chem. Phys.* **57:** 4818–4820.

Koscielska-Kasprzak, K. and Otlewski, J. 2003. Amyloid-forming peptides selected proteolytically from phage display library. *Protein Sci.* **12:** 1675–1685.

Krebs, M.R., Wilkins, D.K., Chung, E.W., Pitkeathly, M.C., Chamberlain, A.K., Zurdo, J., Robinson, C.V., and Dobson, C.M. 2000. Formation and seeding of amyloid fibrils from wild-type hen lysozyme and a peptide fragment from the β-domain. *J. Mol. Biol.* **300:** 541–549.

Lee, S. and Eisenberg, D. 2003. Seeded conversion of recombinant prion protein to a disulfide-bonded oligomer by a reduction-oxidation process. *Nat. Struct. Biol.* **10:** 725–730.

LeVine III, H. 1993. Thioflavine T interaction with synthetic Alzheimer's disease β-amyloid peptides: Detection of amyloid aggregation in solution. *Protein Sci.* **2:** 404–410.

———. 1999. Quantification of β-sheet amyloid fibril structures with thioflavin T. *Methods Enzymol.* **309:** 274–284.

Li, T., Tachibana, K., and Kuroki, M. 2003. Gene transfer with echo-enhanced contrast agents: Comparison between Albunex, Optison, and Levovist in mice—Initial results. *Radiology* **229:** 423–428.

Liu, C., Chu, D., Wideman, R.D., Houliston, R.S., Wong, H.J., and Meiering, E.M. 2001. Thermodynamics of denaturation of hisactophilin, a β-trefoil protein. *Biochemistry* **40:** 3817–3827.

Lobley, A., Whitmore, L., and Wallace, B.A. 2002. DICHROWEB: An interactive website for the analysis of protein secondary structure from circular dichroism spectra. *Bioinformatics* **18:** 211–212.

Lomas, D.A. and Carrell, R.W. 2002. Serpinopathies and the conformational dementias. *Nat. Rev. Genet.* **3:** 759–768.

Mason, T.J. and Peters, D. 2002. *Practical sonochemistry: Uses and applications of ultrasound*, 2nd ed. Horwood Publishing, Chichester, West Sussex, UK.

Meersman, F., Smeller, L., and Heremans, K. 2002. Comparative Fourier transform infrared spectroscopy study of cold-, pressure-, and heat-induced unfolding and aggregation of myoglobin. *Biophys. J.* **82:** 2635–2644.

Morozova-Roche, L.A., Zurdo, J., Spencer, A., Noppe, W., Receveur, V., Archer, D.B., Joniau, M., and Dobson, C.M. 2000. Amyloid fibril formation and seeding by wild-type human lysozyme and its disease-related mutational variants. *J. Struct. Biol.* **130:** 339–351.

Naiki, H., Higuchi, K., Hosokawa, M., and Takeda, T. 1989. Fluorometric determination of amyloid fibrils in vitro using the fluorescent dye, thioflavin T1. *Anal. Biochem.* **177:** 244–249.

Nelson, K.E., Clayton, R.A., Gill, S.R., Gwinn, M.L., Dodson, R.J., Haft, D.H., Hickey, E.K., Peterson, J.D., Nelson, W.C., Ketchum, K.A., et al. 1999. Evidence for lateral gene transfer between Archaea and bacteria from genome sequence of *Thermotoga maritima*. *Nature* **399:** 323–329.

O'Nuallain, B., Williams, A.D., Westermark, P., and Wetzel, R. 2004. Seeding specificity in amyloid growth induced by heterologous fibrils. *J. Biol. Chem.* **279:** 17490–17499.

Provencher, S.W. 1982. CONTIN: A general purpose constrained regularization program for inverting noisy linear algebraic and integral equations. *Comput. Phys. Commun.* **27:** 201–209.

Prusiner, S.B. 1998. Prions. *Proc. Natl. Acad. Sci.* **95:** 13363–13383.

Ramirez-Alvarado, M., Merkel, J.S., and Regan, L. 2000. A systematic exploration of the influence of the protein stability on amyloid fibril formation in vitro. *Proc. Natl. Acad. Sci.* **97:** 8979–8984.

Rochet, J.C. and Lansbury Jr., P.T. 2000. Amyloid fibrillogenesis: Themes and variations. *Curr. Opin. Struct. Biol.* **10:** 60–68.

Saborio, G.P., Permanne, B., and Soto, C. 2001. Sensitive detection of pathological prion protein by cyclic amplification of protein misfolding. *Nature* **411:** 810–813.

Satheeshkumar, K.S. and Jayakumar, R. 2002. Sonication induced sheet formation at the air–water interface. *Chem. Commun. (Camb.)* **19:** 2244–2245.

Scherzinger, E., Lurz, R., Turmaine, M., Mangiarini, L., Hollenbach, B., Hasenbank, R., Bates, G.P., Davies, S.W., Lehrach, H., and Wanker, E.E. 1997. Huntingtin-encoded polyglutamine expansions form amyloid-like protein aggregates in vitro and in vivo. *Cell* **90:** 549–558.

Schmittschmitt, J.P. and Scholtz, J.M. 2003. The role of protein stability, solubility, and net charge in amyloid fibril formation. *Protein Sci.* **12:** 2374–2378.

Senisterra, G.A., Huntley, S.A., Escaravage, M., Sekhar, K.R., Freeman, M.L., Borrelli, M., and Lepock, J.R. 1997. Destabilization of the Ca2+-ATPase of sarcoplasmic reticulum by thiol-specific, heat shock inducers results in thermal denaturation at 37 degrees C. *Biochemistry* **36:** 11002–11011.

Sirangelo, I., Malmo, C., Casillo, M., Mezzogiorno, A., Papa, M., and Irace, G. 2002. Tryptophanyl substitutions in apomyoglobin determine protein aggregation and amyloid-like fibril formation at physiological pH. *J. Biol. Chem.* **277:** 45887–45891 [Epub 42002 Sep 45819].

Soto, C. 2001. Protein misfolding and disease; protein refolding and therapy. *FEBS Lett.* **498:** 204–207.

Soto, C., Saborio, G.P., and Anderes, L. 2002. Cyclic amplification of protein misfolding: Application to prion-related disorders and beyond. *Trends Neurosci.* **25:** 390–394.

Sreerama, N. and Woody, R.W. 2000. Estimation of protein secondary structure from circular dichroism spectra: Comparison of CONTIN, SELCON, and CDSSTR methods with an expanded reference set. *Anal. Biochem.* **287:** 252–260.

Srisailam, S., Wang, H.M., Kumar, T.K., Rajalingam, D., Sivaraja, V., Sheu, H.S., Chang, Y.C., and Yu, C. 2002. Amyloid-like fibril formation in an all β-barrel protein involves the formation of partially structured intermediate(s). *J. Biol. Chem.* **277:** 19027–19036 [Epub 12002 Mar 19024].

Stathopulos, P.B., Rumfeldt, J.A., Scholz, G.A., Irani, R.A., Frey, H.E., Hallewell, R.A., Lepock, J.R., and Meiering, E.M. 2003. Cu/Zn superoxide dismutase mutants associated with amyotrophic lateral sclerosis show enhanced formation of aggregates in vitro. *Proc. Natl. Acad. Sci.* **100:** 7021–7026.

Stefani, M. and Dobson, C.M. 2003. Protein aggregation and aggregate toxicity: New insights into protein folding, misfolding diseases and biological evolution. *J. Mol. Med.* **81:** 678–699.

Sunde, M. and Blake, C. 1997. The structure of amyloid fibrils by electron microscopy and X-ray diffraction. *Adv. Protein Chem.* **50:** 123–159.

Tanaka, M., Machida, Y., Nishikawa, Y., Akagi, T., Morishima, I., Hashikawa, T., Fujisawa, T., and Nukina, N. 2002. The effects of aggregation-inducing motifs on amyloid formation of model proteins related to neurodegenerative diseases. *Biochemistry* **41:** 10277–10286.

Uptain, S.M. and Lindquist, S. 2002. Prions as protein-based genetic elements. *Annu. Rev. Microbiol.* **56:** 703–741.

van de Weert, M., Hennink, W.E., and Jiskoot, W. 2000. Protein instability in poly(lactic-co-glycolic acid) microparticles. *Pharm. Res.* **17:** 1159–1167.

Wei, Y.S., Lin, S.Y., Wang, S.L., Li, M.J., and Cheng, W.T. 2003. Fourier transform IR attenuated total reflectance spectroscopy studies of cysteine-induced changes in secondary conformations of bovine serum albumin after UV-B irradiation. *Biopolymers* **72:** 345–351.

Westermark, G.T., Johnson, K.H., and Westermark, P. 1999. Staining methods for identification of amyloid in tissue. *Methods Enzymol.* **309:** 3–25.

Wolf, M., Wirth, M., Pittner, F., and Gabor, F. 2003. Stabilisation and determination of the biological activity of L-asparaginase in poly(D,L-lactide-co-glycolide) nanospheres. *Int. J. Pharm.* **256:** 141–152.

Wolman, M. and Bubis, J.J. 1965. The cause of the green polarization color of amyloid stained with Congo red. *Histochemie* **4:** 351–356.

Wong, M. and Suslick, K.S. 1995. Sonochemically produced hemoglobin microbubbles. In *Material Research Society Symposium Proceedings* (eds. D.L. Wilcox et al.), Fall 1994, Vol. 372, pp. 89–94. Material Research Society, Pittsburgh, PA.

Wood, R.W. and Loomis, A.L. 1927. The physical and biological effects of high frequency sound waves of great intensity. *Philos. Mag.* **4:** 414–436.

Yee, A., Chang, X., Pineda-Lucena, A., Wu, B., Semesi, A., Le, B., Ramelot, T., Lee, G.M., Bhattacharyya, S., Gutierrez, P., et al. 2002. An NMR approach to structural proteomics. *Proc. Natl. Acad. Sci.* **99:** 1825–1830.

Zambaux, M.F., Bonneaux, F., Gref, R., Dellacherie, E., and Vigneron, C. 1999. Preparation and characterization of protein C-loaded PLA nanoparticles. *J. Controlled Release* **60:** 179–188.